THE THERMODESORPTION OF CO FROM THE Mo(110) SURFACE

N.V. PETROVA, V.D. OSOVSKII, D.YU. BALAKIN, I.N. YAKOVKIN, YU.G. PTUSHINSKII

PACS 68.47.De
©2011

Institute of Physics, Nat. Acad. of Sci. of Ukraine
(46, Prosp. Nauky, Kyiv 03028, Ukraine; e-mail: ptush@iop.kiev.ua)

The problem of the CO adsorption and dissociation on the Mo(110) surface has been studied by means of temperature-programmed desorption (TPD) and density-functional (DFT) calculations. The TPD spectra show a first-order CO desorption, which indicates the desorption from a virgin state, not a recombinative form of desorption. The height of the potential barrier for CO dissociation (2.75 eV), estimated from DFT calculations, substantially exceeds the energy of CO chemisorption on the Mo(110) surface (2.1 eV), which refutes a thermally induced CO dissociation. Monte Carlo simulations of TPD spectra, performed with the use of estimated chemisorption energies, are in good agreement with experiment and demonstrate that the two-peak shape of the spectra can be explained without involving the CO dissociation.

1. Introduction

The simple picture of a molecular form of chemisorption of CO on Mo and W surfaces, suggested in pioneering works [1, 2], was later questioned [3]. Thus, it was suggested that two main peaks, observed in thermal desorption spectroscopy (TDS) (or temperature-programmed desorption, TPD) studies, should be attributed to two different forms of adsorption. Specifically, the low-temperature peak about 300–400 K was explained as the desorption from a molecular CO state (called the α state), while the high-temperature (~ 900–1500 K) peak (the β state) was attributed to the associative desorption of preliminary dissociated CO. It was shown [3] that the low-temperature α state appears only for sufficiently high CO coverages, whereas the multiple β state is characteristic of low coverages and should be attributed to a precursor to the CO dissociation [4].

Surface vibrational studies by electron energy-loss spectroscopy (EELS) for CO adsorbed on the W(110), Mo(110), and Mo(100) surfaces [5-7] revealed an unusually low C–O stretching frequency (~ 1000–1100 cm^{-1}). This mode disappeared upon annealing to 230 K, so it was suggested that CO should dissociate already at ~ 200 K. Accordingly, Umbach and Menzel [8] observed the CO dissociation on W(110) at temperatures between 200 and 300 K, with a surprisingly small activation energy (≈ 21 kJ/mol). However, no such precursor state was detected in the infrared reflection absorption spectroscopy (IRAS) study of the adsorption of CO on clean and O-, C-, and H-precovered Mo(110) surfaces [9].

The studies [10–12] based on angle-resolved ultraviolet photoemission spectroscopy (UPS), as well as the near-edge X-ray absorption fine structure, indicate that, at low coverages, CO molecules on W and Mo surfaces are tilted (the β state), while, at sufficiently high coverages, they are oriented perpendicularly to the surface with the C atom down (the α state). Using the high-resolution core-level spectroscopy and UPS for the CO adsorption on Mo(110), Jaworowski *et al.* [12] suggested a thermally activated dissociation of CO molecules. Then, in a recent DFT study [13], the thermal dissociation of CO on Mo(110) was adopted as an experimentally established fact. Similar conclusions were derived also from TDS studies for CO on Mo(110) [14] and Mo(112) [15]. In line with the established concept, the peaks about 700–900 K in TPD spectra for CO on Mo(112) [15] were attributed to the recombinative CO desorption. In fact, however, neither experiments nor theoretical studies cited above have proved the thermal dissociation of CO on W or Mo surfaces, which is mandatory for the subsequent associative desorption. In particular, the CO dissociation was suggested to explain the absence of the CO stretching mode in EELS at low coverages, but this result hardly could be a decisive argument, because the dipole selection rule for a CO molecule parallel to the surface will cause the elimination of this mode. The UPS results have shown, in turn, that the β state corresponds to a tilted orientation of CO, but not to dissociated CO molecules. Thus, the photoemission spectra for CO on W(110) and Mo(110) [16], as well as the first-order desorption kinetics for the β – state, were convincingly interpreted as the absence of CO dissociation.

In turn, on a Mo(112) surface, the absence of CO dissociation was suggested basing on DFT calculations of the binding (chemisorption) energies, local densities of

states (LDOS), and CO vibrational frequencies for various configurations of equilibrated adlayers [17]. It was shown, by means of Monte Carlo simulations, that the two-peak shape of TPD spectra for CO can be explained with the estimated CO chemisorption energies for low and high coverages, that is, without involving the CO dissociation. In the present paper, we revisit the problem of the CO dissociation on transition metal surfaces. The performed TPD study and DFT calculations, as well as Monte Carlo simulations of desorption spectra, show that the thermally induced CO dissociation on Mo(110) is improbable.

2. Experimental and Theoretical Methods

The experiments were performed in an ultrahigh-vacuum system with a base pressure of $\sim 10^{-11}$ Torr, equipped with low energy electron diffraction (LEED) and a quadrupole mass-spectrometer for TPD studies. The Mo(110) samples were cleaned by heating at 1600 K in the oxygen atmosphere of 1×10^{-6} Torr, followed by several flashes to 2100 K. The sample was cooled using an N_2 cryogenic system which was connected to the sample with a Cu rod. For the CO deposition, the system was backfilled with CO. The sample temperature was measured using a W–W/Re thermocouple, spot-welded to the back surface of the sample. The heating rates in TPD experiments were 10–40 K·s^{-1}.

The DFT semirelativistic calculations using the repeat-slab model and the plane-waves expansion of a wave function were carried out with ABINIT code [18], using the Troullier-Martins [19] norm-conserving pseudopotentials and generalized gradient approximation (GGA) with a PBE [20] exchange-correlation functional. Because of nodeless 2p valent orbitals, the norm-conserving pseudopotential for oxygen is quite hard, i.e. requires a high cutoff energy. Thus, the well-converged (about 1 mHa (0.027 eV)) values of total energies were obtained with the 34-Ha cutoff energy. The quality of the pseudopotentials was estimated by calculations of the binding energies for free O_2 and CO molecules (taking the triplet ground state of O atoms into account) [17]. The efficiency of the Brillouin zone sampling, using various k-point lattices, was carefully verified by increasing the number of k-points until the required 0.002-Ha convergence of total energies and the about 0.02-Å accuracy of atomic positions were achieved (for rectangular 1×1 lattices, the $4\times4\times1$ Monkhorst–Pack [21] set was found sufficient).

The surface unit cell was chosen to be 2×1 or, when appropriate, 1×1. The vacuum gap between the 5-layer
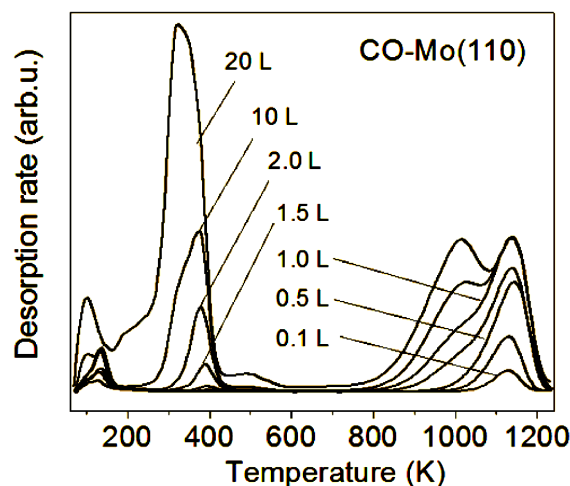

Fig. 1. Desorption spectra obtained for various Mo(110) exposures (Langmuir) in the CO atmosphere at $T = 90$ K. The rate of temperature increase was 40 K·s^{-1}

Mo(110) slabs was about the thickness of slabs. Before depositing CO, the slabs were relaxed, that is, all atoms were allowed to adjust their position using the Broyden optimization procedure. Then, CO molecules were adsorbed in various sites on one side of the slab. The positions of CO molecules and Mo atoms were optimized, so that the binding energies defined as $-E_b = E - E_{Mo} - E_{CO}$, where E, E_{CO}, and E_{Mo} are total energies of the adsorption system, CO molecule, and the substrate unit cell, respectively, were determined with account for the relaxation of clean surfaces, as well as the CO-induced surface relaxation.

3. Results and Discussion

3.1. TPD spectra

Desorption spectra obtained for various Mo(110) exposures in the CO atmosphere at room temperature are shown in Fig. 1. The 1130-K peak appears already for the ~ 0.1 L exposure and increases with the further deposition of CO, but its position remains constant. This feature is characteristic of the first-order type of desorption, that is, of virgin CO molecules. In other words, the behavior of the high-temperature peak (the β peak [2–4]) does not resemble the associative desorption of CO suggested in numerous studies (for instance, [2–15]), but it is perfectly consistent with conclusions derived from the TPD study for CO on W(110) [16].

For CO exposures above 1.5 L, the shoulder on the 1130-K peak gradually transforms to the peak at ~ 1000 K. At the further exposure, there appears a low-
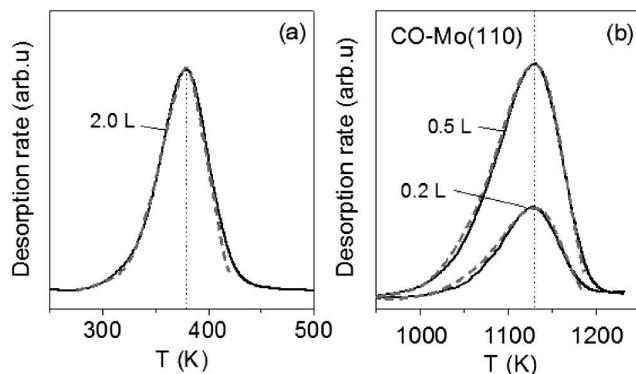
Fig. 2. Approximation of TPD spectra (solid black lines) using the first-order Polanyi–Wigner equation (dashed lines). The best fit is achieved with $\nu = 2 \times 10^9$ s^{-1} and $E_d = 0.7$ eV for the 380-K peak (a) and with the same $\nu = 2 \times 10^9$ s^{-1} and $E_d = 2.1$ eV for the 1130-K peak (b)

temperature peak at ~ 380 K (the α peak [2–4]) which is usually attributed to the molecular (virgin) desorption. Hence, while the obtained spectra are consistent with similar TPD results for CO on Mo(110) [14], Mo(112) [15], and W(110) [16], we suggest that the behavior of the high-temperature peak reveals the molecular (non-recombinative) desorption of CO from Mo(110), as it was found for CO/W(110) [16].

It is generally believed that a proper analysis of thermodesorption spectra allows for a reasonable estimate of the energy of desorption E_d and the frequency factor ν which determine the rate R of the first-order ($n = 1$) or the second-order (associative, $n = 2$) desorption in the Polanyi–Wigner equation

$$R = -\frac{d\theta}{dt} = \nu\theta^n \exp\left(\frac{-E_d}{kT}\right). \tag{1}$$

For a linear dependence of the temperature on time, $T = T_0 + \beta t$, one can explore either the Redhead [22] or King [23] formalism to evaluate both E_d and ν. However, the values thus obtained can differ dramatically (see, e.g., [24, 25]).

To our view, the best way to reliable estimates of E_d and ν is a direct application of the Polanyi–Wigner formula (1), which can be performed by fitting the model spectra calculated for various E_d and ν to experimental TPD spectra [25]. In particular, both the 380- and 1130-K peaks in the spectra of the CO desorption from Mo(110) can be well approximated by the first-order Polanyi–Wigner equation with $\nu = 2 \times 10^9$ s^{-1} and the desorption energies $E_d = 0.7$ and 2.1 eV, respectively (Fig. 2). The same shapes of the experimental and model spectral peaks ultimately indicate the first-order
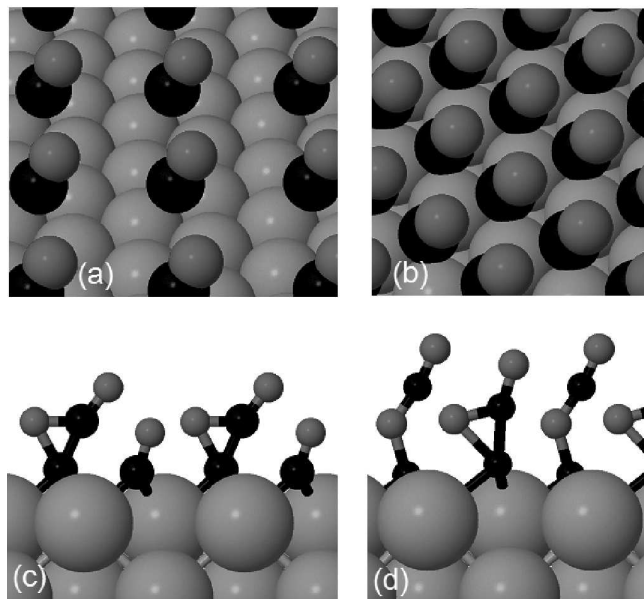

Fig. 3. Favorable CO structures on Mo(110) at $\theta = 0.25$ (a), 1.0 (b), 1.5 (c), and 2.0 (d). Carbon atoms are shown black, O red, and Mo blue. In the first layer, CO molecules are tilted and occupy nearly threefold hollow sites. CO molecules of the second layer are bound to CO of the first layer

desorption kinetics characteristic of the molecular (non-recombinative) form of desorption. With increase in the coverage, both 1130- and 380-K peaks get significantly transformed, which is indicative of lateral interactions more pronounced in denser layers, as discussed below.

3.2. DFT calculations of binding energies

On Mo(110), favorable adsorption positions for CO molecules could be atop surface Mo atoms, in short-bridge and long-bridge sites, and in triply coordinated hollow sites. The most favorable for CO molecules in a (2×2) structure ($\theta = 0.25$) are found to be the nearly hollow sites (Fig. 3,a). The CO molecules are tilted by $\sim 30°$. The estimated binding energy of CO in these positions is of 2.0 eV. The long-bridge sites are less favorable by ~ 0.2 eV, the on-top sites – by ~ 0.3 eV, while the short-bridge sites are found to be unfavorable for all CO coverages.

The hollow sites remain favorable also for $\theta = 1.0$. Therefore, for coverages up to 1 ML, CO molecules will occupy predominantly these sites (Fig. 3,b). The distance between neighboring CO molecules in the forming p(1×1) CO structure is 2.73 Å. At these distances, the lateral interaction (repulsive) becomes significant, so that the binding energy decreases (by ~ 0.2 eV) with re-
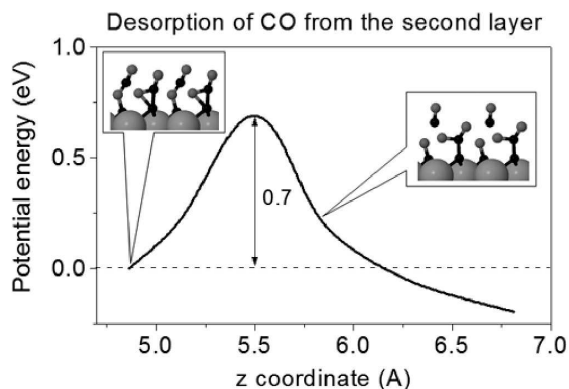
Fig. 4. Potential energy changes during the CO desorption from the second layer

Fig. 5. Potential barrier for the CO dissociation on Mo(110)

spect to that for $\theta = 0.5$, and the tilting angle decreases to 24°.

The estimated lateral interaction can explain the split of the high-temperature TPD peak for high CO coverages (as illustrated below by Monte Carlo simulations), but definitely not the appearance of the 380-K peak that corresponds to the 0.7-eV binding energy. The low-temperature peak appears only for sufficiently high CO exposures and, as follows from the estimate of a binding energy for the p(1×1) CO structure ($\theta = 1.0$), should be attributed to the desorption from the second CO layer.

The formation of a CO bilayer was modeled for $\theta = 1.5$ and 2.0. The optimized structures can be considered as C_2O_2 complexes (the formation of C=C=O species was observed also for the CO adsorption atop the surface carbon on the C-terminated α-Mo$_2$C(0001) [26]) and curved C–O–C–O chains (Fig. 3,c,d). The desorption of a CO molecule corresponds to the breaking of the bond between two CO fragments, so that the upper CO molecule of the chain desorbs, while the other remains on the surface. However, a routine estimate of the binding energy gives negative values of E_d, which means that the second layer of CO can remain on the surface only due to short-range bonds with the first CO layer.

The CO desorption from the second layer was modeled by a stepwise movement of an upper CO molecule along the normal (**z** coordinate) away from the surface. For each reaction step, only the **z** coordinate of the upper O was kept fixed, while positions of the other C and O atoms were optimized. The barrier for desorption was estimated as the potential energy difference between the initial state and the state at the barrier top (Fig. 4). It should be noted that the thus obtained value $E_d = 0.7$ eV is perfectly consistent with the position of the 380-K peak in TPD spectra.
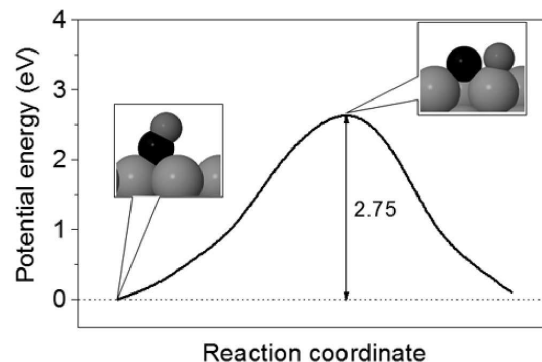
3.3. The potential barrier for CO dissociation

To estimate the potential barrier for the CO dissociation, which might be possible at low coverages, we have simulated the reaction path for the dissociation of CO molecules by moving the O atom in the [001] direction (**x** coordinate). For each reaction step, both C and O were allowed to relax along the **z** coordinate, while the (**x** coordinates were kept fixed until the attraction between C and O persisted. At the vertex of the potential plot (the transition state) (Fig. 5), the positions of C and O were optimized to eliminate net forces on the atoms, and the potential barrier for dissociation was estimated as the difference between the energies of the initial and transition states. On moving the O atom to the left from the critical point, C and O spontaneously recombine, thus forming a CO molecule in the β state, while on moving the O atom to the right, the appearing lateral repulsion results in the dissociation. It should be noted that the transition point was found "by hand," i.e., without involving the vibrational analysis, which is quite complicated and time consuming in this case. Nonetheless, the appearance of backward forces on shifting O atoms indicates that the vertex of the barrier corresponds, indeed, to a saddle point on the potential energy surface.

The most important result of these calculations is that the estimated potential barrier for the dissociation, 2.75 eV, exceeds substantially the estimated energy of CO desorption (2.0 eV). This means that, on heating, CO molecules would rather desorb from the surface than dissociate. Therefore, the high-temperature (β) peak in TPD spectra cannot be attributed to consecutive dissociation-association processes.

3.4. Monte Carlo simulations

The Monte Carlo simulations of the thermodesorption were performed using a routine "real-time" algo-
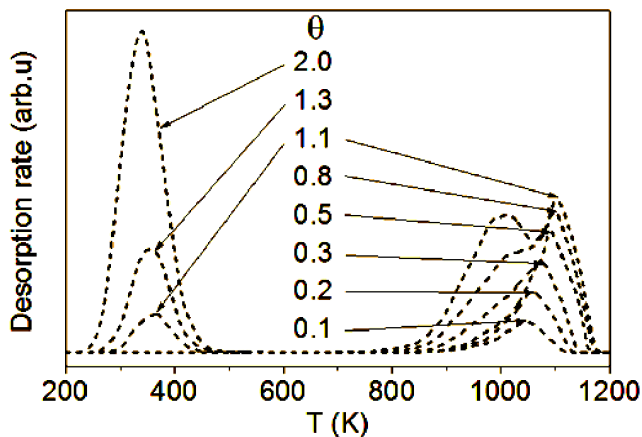
Fig. 6. Model TPD spectra obtained by kinetic Monte Carlo simulations for various initial CO coverages. The spectra were simulated with $\nu = 2 \times 10^9$ s^{-1} and binding energies of 2.1 and 0.7 eV for CO molecules in the first and second layers, respectively

rithm [14, 17, 25, 27, 28]. The temperature was increased stepwise, and the number of desorption attempts for each step was determined by the time interval dependent on β. The probability W of the desorption of a molecule per second was defined as $W = \nu \exp(-(E_d - E_{int})/kT)$, that is, the energy of desorption was expressed as the sum of the binding energy E_b and the energy of lateral interactions E_{int} (~ 0.2 eV for the nearest neighboring CO) estimated from the difference of binding energies calculated for low ($\theta = 0.25$) and high ($\theta = 1.0$) coverages. The frequency factor $\nu = 2 \times 10^9$ s^{-1} was taken from the experiment (see Fig. 2).

The model TPD spectra obtained by kinetic Monte Carlo simulations for various initial CO coverages are shown in Fig. 6. The spectra were obtained with binding energies of 2.1 and 0.7 eV for CO in the first and second layers, respectively. These energies are perfectly consistent with the values derived from the analysis of experimental spectra using the Polanyi–Wigner equation (see Fig. 2) (it should be noted that the DFT/GGA gives a somewhat underestimated binding energy of 2.0 eV at $\theta = 0.25$). In agreement with experiment, the spectra have two main peaks: at ~ 1100 K (β phase) and, for coverages above 1.0 ML, 380 K (α phase). For $\theta < 1$ ML, only the β phase is formed, and the peak gradually moves toward higher temperatures (which is due to the high (40 K·s^{-1}) rate of temperature increase, as it was verified in simulations with various rates). The repulsive lateral interaction modifies the shape of the peak, so that it becomes wider at $\theta = 1.0$ ML and splits into two

peaks at ~ 1000 and 1130 K. The α peak appears, in turn, at filling the second layer, and an apparent shift of its vertex to lower temperatures originates by lateral interactions (related close-spaced peaks are not resolved again, because of a high rate of temperature increase).

Hence, the present results of Monte Carlo simulations demonstrate that the TPD spectra for CO on Mo(110) can be explained by the first-order (molecular) desorption from the second and the first adsorbed layers. Indeed, both low- (α) and high-temperature (β) desorption peaks in the TPD spectra are well reproduced in the model, and the high-temperature peak is originated not by the consecutive dissociation-recombination of CO, but by virgin CO desorbing from the first layer. The low-temperature peak corresponds, in turn, to the desorption from the second layer.

4. Conclusion

The results of the present study agree well with a general picture of CO adsorption on Mo surfaces. The main conclusion which can be derived from the present calculations of chemisorption energies and the Monte Carlo simulations is that there is no need to invoke a ghost dissociation of CO for the explanation of TPD spectra. The first-order kinetics of CO desorption indicates that CO desorbs from a "virgin" state. The height of the potential barrier for the dissociation (2.75 eV) estimated from DFT calculations exceeds substantially the energy of CO chemisorption (2.1 eV), which makes the thermally induced CO dissociation on Mo improbable. Hence, the β state cannot be attributed to the precursor to the dissociation – because CO on Mo does not dissociate at all.

1. G. Ehrlich, T.W. Hickmott, and F.G. Hudda, J. Chem. Phys. **28**, 506 (1958); G. Ehrlich, J. Chem. Phys. **34**, 39 (1961).

2. R. Klein, J. Chem. Phys. **31**, 1306 (1959); L.W. Swanson and R. Gomer, J. Chem. Phys. **39**, 2813 (1963); C. Kohrt and R. Gomer, Surf. Sci. **40**, 71 (1973).

3. C.G. Goymour and D.A. King, J. Chem. Soc. Faraday Trans. 1 **69**, 736 (1973); Surf. Sci. **35**, 246 (1973).

4. C. Wang and R. Gomer, Surf. Sci. **90**, 10 (1979).

5. J.E. Houston, Surf. Sci. **255**, 303 (1991).

6. J.G. Chen, M.L. Colaianni, W.H. Weinberg, and J.T. Yates, jr., Chem. Phys. Lett. **177**, 113 (1991).

7. F. Zaera, E. Kollin, and J.L. Gland, Chem. Phys. Lett. **121**, 454 (1985).

8. E. Umbach and D. Menzel, Surf. Sci. **135**, 199 (1983).

9. J.-W. He, W.K. Kuhn, and D.W. Goodman, Surf. Sci. **262**, 351 (1992).

10. J.W. Davenport, Phys. Rev. Lett. **36**, 945 (1976); R.J. Smith, J.A. Anderson, and G.J. Lepeyre, Phys. Rev. Lett. **37**, 1081 (1976); D.E. Eastman and J.K. Cashion, Phys. Rev. Lett. **27**, 1520 (1971); T. Gustafsson, E.W. Plummer, D.E. Eastman, and J.L. Freeouf, Sol. St. Commun. **17**, 391 (1975).

11. F. Zaera, J.P. Fulmer, and W.T. Tysoe, J. Vac. Sci. Technol. A **6**, 875 (1988).

12. A.J. Jaworowski, M. Smedh, M. Borg, A. Sandell, A. Beutler, S.L. Sorensen, E. Lundgren, and J.N. Andersen, Surf. Sci. **492**, 185 (2001).

13. Z. Ji and J.-Q. Li, J. Phys. Chem. B **110**, 18363 (2006).

14. M. Juel and S. Raaen, Philos. Magaz. **83**, 2475 (2003).

15. K. Fukui, T. Aruga, and Y. Iwasawa, Surf. Sci. **281**, 241 (1993).

16. T. Yang, H. Jee, J.-H. Boo, H.S. Han, G.H. Lee, Y.D. Kim, and S.-B. Lee, Bull. Korean Chem. Soc. **29**, 1115 (2008); Y.D. Kim, J.-H. Boo, and S.-B. Lee, Surf. Sci. **603**, 1434 (2009).

17. I.N. Yakovkin and N.V. Petrova, J. Chem. Phys. **130**, 174714 (2009).

18. X. Gonze, J.-M. Beuken, R. Caracas, F. Detraux, M. Fuchs, G.-M. Rignanese, L. Sindic, M. Verstraete, G. Zerah, F. Jollet, M. Torrent, A. Roy, M. Mikami, Ph. Ghosez, J.-Y. Raty, and D.C. Allan, Comput. Mat. Sci. **25**, 478 (2002).

19. N. Troullier and J.L. Martins, Phys. Rev. B **43**, 1993 (1991).

20. J.P. Perdew, K. Burke, and M. Ernzerhof, Phys. Rev. Lett. **77**, 3865 (1996).

21. H.J. Monkhorst and J.D. Pack, Phys. Rev. B **13**, 5188 (1976).

22. P.A. Redhead, Vacuum **12**, 203 (1962).

23. D.A. King, Surf. Sci. **47**, 384 (1975).

24. H. Shimizu, K. Christmann, G. Ertl, and J. Catal. **61**, 412 (1980); J.A. Schwarz, Surf. Sci. **87**, 525 (1979); P. Feulner and D. Menzel, Surf. Sci. **154**, 465 (1985).

25. N.V. Petrova and I.N. Yakovkin, Eur. Phys. J. B **63**, 17 (2008).

26. J. Ren, H. Chun-Fang, J. Wang, L. Yong-Wang, and H. Jiao, Surf. Sci. **59**, 212 (2005).

27. B. Meng and W. Y. Weinberg, J. Chem. Phys. **100**, 5280 (1994); C. Stampfl, H.J. Kreuzer, S.H. Payne, H. Pfnür, M. Scheffler, Phys. Rev. Lett. **83**, 2993 (1999); D.L.S. Nieskens, A.P. van Bavel, and J.W. Niemantsverdriet, Surf. Sci. **546**, 159 (2003).

28. N.V. Petrova and I.N. Yakovkin, Phys. Rev. B **76**, 205401 (2007); Eur. Phys. J. B **58**, 257 (2007).

ТЕРМОДЕСОРБЦІЯ CO З ПОВЕРХНІ Mo(110)

Н.В. Петрова, В.Д. Осовський, Д.Ю. Балакін, І.М. Яковкін, Ю.Г. Птушинський

Р е з ю м е

Методами температурно-програмованої десорбції (TPD) та теорії функціонала густини (DFT) досліджено проблему адсорбції та дисоціації CO на поверхні Mo(110). Спектри TPD виявили перший порядок десорбції CO, що свідчить про десорбцію з молекулярного стану, але не про асоціативну форму десорбції. Висота потенціального бар'єра для дисоціації CO (2,75 еВ), отримана з DFT розрахунків, суттєво перевищує енергію хемосорбції CO на поверхні Mo(110) (2,1 еВ), що включає термічну дисоціацію CO. Монте-Карло моделювання спектра TPD з врахуванням оцінених енергій хемосорбції добре узгоджується з експериментом та демонструє двопікову форму спектра термодесорбції, яка пояснюється без залучення дисоціації CO.